Actin isovariant ACT7 regulates root meristem development in Arabidopsis through modulating auxin and ethylene responses

Takahiro Numata[1§], Kenji Sugita[1§], Arifa Ahamed Rahman[2] and Abidur Rahman[1,2,3*]

[1]Department of Plant Bio Sciences, Faculty of Agriculture, Iwate University, Morioka 020-8550, Japan

[2] The United Graduate School of Agricultural Sciences, Iwate University, Morioka 020-8550, Japan

[3]Agri-Innovation Center, Iwate University, Morioka 020-8550, Japan

[*]Corresponding author: Email: abidur@iwate-u.ac.jp

[§] These authors contributed equally.

Running title: Actin isovariant specific regulation of root meristem development

Abstract

Meristem, which sustains a reservoir of niche cells at its apex, is the most functionally dynamic part in a plant body. The shaping of the meristem requires constant cell division and cell elongation, that are regulated by hormones and cell cytoskeletal components, actin. Although the roles of hormones in regulating meristem development have been extensively studied, the role of actin in this process is still elusive. Using the single and double mutants of the vegetative class actin, we demonstrate that ACT7 plays a primary role in regulating the root meristem development. In absence of ACT7, but not ACT8 and ACT2, cellular depolymerization of actin is observed. Consistently, *act7* mutant shows reduced cell division, cell elongation and meristem length. Intracellular distribution and trafficking of auxin transport proteins in the actin mutants revealed that ACT7 specifically functions in root meristem to facilitate the trafficking of auxin efflux carriers PIN1 and PIN2, and consequently the transport of auxin. Compared with *act7*, *act7act8* double mutant shows slightly enhanced phenotypic response and altered intracellular trafficking. The altered distribution of auxin in *act7* and *act7act8* affects the roots response to ethylene but not to cytokinin. Collectively, our results suggest that Arabidopsis root meristem development is primarily controlled through actin isovariant ACT7 mediated modulation of auxin-ethylene response.

Introduction:

Meristem, which sustains a reservoir of niche cells at its apex, is the most functionally dynamic part in a plant body. The formation of meristem is essential for plant growth and development, and this process is regulated by interaction of multiple signaling networks, including receptor kinase signaling, transcriptional signaling, and hormonal signaling and transport (Barton, 2010). The shaping up of the meristem requires a constant cell division and cell elongation of the source stem cells. Both the hormones and cell cytoskeletal components have been attributed to regulate the cell division and cell elongation processes in the meristem cells (Rahman et al., 2007)

Several studies have revealed that the asymmetric cell division and expansion processes are controlled by a dynamic cell cytoskeleton consisting dozens of interacting proteins that responds to both environmental and developmental cues (Clayton and Lloyd, 1985; Lloyd, 1991; Baluška et al., 2001; Kandasamy et al., 2007). Actin, a highly conserved and ubiquitous protein, is a major component of the cell cytoskeleton and essential for various important cellular processes, including cell division and cytokinesis, establishment of cell polarity, cell division plane determination, cell shape, cell polarity, protein trafficking, cytoplasmic streaming, organelle movement and tip growth (Staiger and Schliwa, 1987; Smith and Oppenheimer, 2005; Staiger and Blanchoin, 2006; Kandasamy et al., 2009; Pollard and Cooper, 2009). Plants have multiple actin isoforms encoded by large ancient gene families (McLean et al., 1990; Meagher, 1991). In Arabidopsis, there are eight actin isovariants, which are grouped in two ancient classes, reproductive and vegetative classes (Kandasamy et al., 2009), supplementary Fig. 1). Several lines of evidence strongly suggest that the two major classes of plant actin isovariants are functionally distinct. The vegetative actin isovariants, expressed in young tissues play role in meristem development, while the plants reproduction is regulated by reproductive class of actin (Gilliland et al., 2002). Recent experimental approaches using different isovariants of actin further confirm that the three vegetative actin isovariants play distinct subclass specific roles during plant morphogenesis (Gilliland et al., 2003; Kandasamy et al., 2009). For instance, among three vegetative actin, ACT7 has been shown to be preferentially and strongly expressed in all young and developing vegetative tissue including root meristem, and *ACT7* expression is strongly altered by plant hormone auxin and several external stimuli (McDowell et al., 1996). It also has been shown that ACT7 regulates the germination, root growth, epidermal cell specification, and root architecture (Gilliland et al., 2003; Kandasamy et al., 2009). On the other hand, ACT2 and ACT8 regulate bulge site selection,

root hair growth, and leaf morphology (Ringli et al., 2002; Nishimura et al., 2003; Kandasamy et al., 2009; Vaškebová et al., 2018).

Another major regulator of plant growth and development is hormone. The root meristem development is controlled by a complex regulatory network of hormones involving auxin, ethylene and cytokinin (Bertell and Eliasson, 1992; Liu et al., 2017). Auxin plays a central role in this regulatory network through interacting with other two hormones (Rahman, 2013). Polar auxin driven formation of robust auxin gradient is an absolute requirement for root meristem development (Benková et al., 2003; Friml, 2003; Grieneisen et al., 2007). It has also been shown that root-produced auxin is required for root stem cell niche maintenance (Brumos et al., 2018). Collectively, local auxin biosynthesis and auxin transport act redundantly to establish and maintain the robust auxin maxima critical for root meristem development. This auxin maxima at the root tip, in combination with separable roles of auxin in cell division and cell expansion, can explain the root meristem development.

Cytokinin has been shown to be another major regulator to control the meristem activity. Experiments resulting in depletion of cytokinin in the root meristem along with cytokinin mutants analyses revealed that cytokinin functions at the transition zone to control the cell differentiation rate (Dello Ioio et al., 2007; Müller and Sheen, 2007; Dello Ioio et al., 2008). The classical antagonistic interaction between cytokinin and auxin that regulates the root and shoot organogenesis has been extended to the root meristem development and shown to be regulated through a simple regulatory circuit converging on the *Aux/IAA* gene *SHY2/IAA3*, and polar auxin transport mediated auxin gradient (Dello Ioio et al., 2008a; Chapman and Estelle, 2009; Růzička et al., 2009; Moubayidin et al., 2010)

Ethylene also plays an important role in root meristem development. Cell division in quiescent cells, which act as a source of stem cells, has been shown to be modulated by Ethylene. The ethylene-induced new cells in the quiescent center (QC) express QC specific genes that can repress differentiation of surrounding cells (Ortega-Martínez et al., 2007). Consistently, constitutive triple response mutant *ctr1* show reduced meristematic cell division and meristem size, while the ethylene insensitive mutant *ein2* shows opposite phenotype. Exogenous application of ethylene also mimics the constitutive phenotype (Street et al., 2015). Auxin-ethylene interaction for root growth and development has been well studied (Rahman et al., 2001; Rahman et al., 2002;

Stepanova et al., 2005; Muday et al., 2012). Reduction in intracellular auxin level results in ethylene insensitivity that affects the root morphology. The ethylene sensitivity and the root morphology could be restored by increasing the intracellular auxin level using exogenous auxin (Rahman et al., 2001). Conversely, ethylene has been shown to promote auxin synthesis and transport in root tips resulting in formation of a second auxin maximum in the root elongation zone and alteration in root meristem development (Růzicka et al., 2007; Stepanova et al., 2007; Swarup et al., 2007; Stepanova et al., 2008). Ethylene-induced local auxin synthesis is achieved by upstream tryptophan biosynthesis enzyme genes *WEI2/ ASA1 and WEI7/ ASB1* genes that are precisely regulated by ethylene (Stepanova et al., 2005; Okamoto et al., 2008). This local auxin synthesis by ethylene also alters the auxin gradient in the root tip and affects the root meristem development (Okamoto et al., 2008). Furthermore, it has been shown that *SHY2/IAA3* is a point of convergence for both ethylene and cytokinin in negatively regulating cell proliferation (Street et al., 2015).

Although the cell division and cell proliferation that control the meristem development are regulated by both hormones and cell cytoskeleton component actin, the integrating mechanisms of these two components remain elusive. It has been shown that mutations in vegetative actin isovariant genes result in alteration in root morphology and root development (Ringli et al., 2002; Gilliland et al., 2003; Nishimura et al., 2003; Kandasamy et al., 2009; Vaškebová et al., 2018). However, it remains obscure how the isovariant specific actin regulates the root developmental process. In the present study, using a combinatorial approach of physiology, genetics, and cell biology we demonstrate that root meristem development is primarily controlled by actin isovariant ACT7. In absence of ACT7, but not ACT8 and ACT2, cellular depolymerization of actin was observed. Consistently, *act7* mutant showed reduced cell division, cell elongation and meristem length. Intracellular distribution and trafficking of auxin transport proteins in the actin mutants revealed that ACT7 specifically functions in root meristem to facilitate the trafficking of auxin efflux carriers PIN1 and PIN2, and consequently the transport of auxin. Compared with *act7*, *act7act8* double mutant shows slightly enhanced phenotypic response and altered intracellular trafficking. The altered distribution of auxin in *act7* and *act7act8* affects the roots response to ethylene but not to cytokinin. Collectively, our results suggest that Arabidopsis root meristem development is primarily controlled through actin isovariant ACT7 mediated modulation of auxin-ethylene response.

Results:

Root actin organization is primarily regulated by actin isovariant ACT7

To investigate the effect of mutations in vegetative actin genes on intracellular actin structure and organization, we observed the actin structure using both immunostaining and live cell imaging approaches. Actin in elongation zone was observed as the structure of the actin in this zone is most reliable to compare. For live cell imaging, actin mutants were crossed with the actin marker line ABD2-GFP (Actin Binding Domain 2 of Fimbrin protein, Wang et al., 2007) and homozygous lines were selected. The actin structure observed by both the approaches was largely similar. In wild type, actin labeled in elongation zone showed fine filamentous cable like structure (Fig. 1A). Actin filament structure in *act2-1 and act8-2* showed normal actin filaments like wild-type (Figs. 1B, 1D). Comparable results were observed with live cell imaging using actin marker lines (Figs. 1G, 1H, 1J). Loss of both ACT2 and ACT8 did not affect the structure of the actin. Although a slight reduction of actin was observed in immunostained samples, the actin structure in *act2act8*ABD2-GFP lines was like wild-type (Figs. 1E and 1K). In contrast, loss of ACT7 drastically affected actin structure, showing segmented and aberrant actin cables (Figs. 1C, 1I). This fragmented and aberrant actin phenotype was slightly more enhanced in *act7act8* double mutant (Figs. 1F; 1L), suggesting that among the actin isovariants, ACT7 plays a key role in determining the root actin structure.

Intracellular actin organization affects the primary root elongation and meristem development

To understand whether the change in the actin structure observed in actin mutants correlate the plant growth and development, next we performed the comparative analysis of these actin isovariant mutants against wild-type for root elongation, meristem size, cell production rate and cell length (Fig. 2, Table 1). Seedling phenotype of single and double mutants revealed that the primary root elongation is severely compromised in the mutants where ACT7 is mutated. Both the *act7* and *act7act8* mutants showed dwarf root phenotype, while the wild-type like or a slight increase in the primary root elongation was observed in *act2*, *act8* and *act2act8* (Fig. 2A). The *act7act8* double mutant showed a little more severe phenotype than *act7-4* single mutant (Fig. 2A). These phenotypic observations suggest that the intracellular actin organization directly influences

the primary root elongation and further reveals that that ACT7 is the primary regulator of this process.

Root elongation is regulated by both cell division and cell elongation and consequently linked to the root meristem size and development (Beemster and Baskin, 1998). The assessment of meristem length in vegetative class actin isovariant mutants revealed that dwarf root phenotype observed in *act7* and *act7act8* mutants is a consequence of reduced meristem development (Figs. 2B, 2C). In contrast, *act2* and *act2act8* showed a slight but statistically significant increase in meristem length (Figs. 2B, 2C). Taken together, these results suggest that actin isovariants regulate root meristem development separately. ACT7 plays role in primary root meristem development as a positive regulator, while ACT2 may function as negative regulator.

To further understand how actin isovariant regulates the root meristem size, we took a kinematic approach as described earlier (Rahman et al., 2007). The root elongation rate and the length of the newly matured cortical cells were measured in wild type, *act2-1*, *act8-2*, *act7-4*, *act2act8*, and *act7act8* mutants. The ratio of mature cell length to root elongation rate gives the time required to produce one cortical cell (per cell file); which is also defined as the cell production rate (Silk et al., 1989). The cell production rate represents the output of the meristem reflecting both the number of dividing cells and their rates of division (Beemster and Baskin, 1998; Rahman et al., 2007). Kinematic analysis revealed that that loss of ACT7 results in a large reduction in root elongation, cell length, and subsequently lower cell production rate (Table 1). Further, the double mutant *act7act8*, which shows a little more severe root phenotype than *act7-4*, also shows a reduced cell division activity compared with *act7-4*. These data suggest that ACT7 plays a dominant role in regulating the cell division activity at primary root meristem. Loss of ACT8 alone does not change the cell production activity but loss of ACT8 in conjunction with ACT7 affect the roots cell division ability negatively, consistent with the idea that actin plays a significant role in controlling the cell division and ACT7 isovariant is the primary regulator of this process (Table 1). On the other hand, loss of ACT2 results in an increased cell production rate although the cell length is not affected. The double mutant *act2act8* also shows a similar trend (Table 1). Taken together, these results suggest that the root meristem development is regulated by isovariant specific actin, and ACT7 is the primary regulator of this process.

ACT7 modulates the intracellular trafficking of a subset of auxin transport proteins

In eukaryotic cells, targeting of proteins to specific organelles or to and from membrane is regulated by protein trafficking, an important process for cellular activity and growth. It is generally assumed that the cytoskeleton component actin acts like a network of tracks for the movement of vesicles between cellular compartments (Simon and Pon, 1996; Huang et al., 1999; Nebenführ and Staehelin, 2001; Kim et al., 2005). Polar transport and the formation of auxin gradient in the root meristem largely relies on the intracellular trafficking of PIN proteins through which the proteins are correctly localized to the membrane (Feraru and Friml, 2008), and this localization of PIN efflux carriers has been shown to be actin dependent. Disruption in actin structure results in reduced trafficking of these proteins to and from the membrane and subsequently affects their asymmetric localization (Geldner et al., 2001; Muday and Murphy, 2002; Rahman et al., 2007; Kleine-Vehn and Friml, 2008). Since polar auxin mediated auxin gradient at root tip plays a major role in regulating root meristem development and actin mutants show altered root meristem size, we hypothesized that the observed meristem phenotype in these mutants may be linked to the altered trafficking of the auxin transporters. To test this hypothesis, we investigated the intracellular localization of the PIN proteins in actin mutant backgrounds. Live cell imaging analyses using translationally fused GFP with PIN proteins in various actin mutant backgrounds revealed that the loss of actin does not alter the polar localization of these proteins (Figs. 3-5). However, the intracellular trafficking of PIN1 and PIN2 is found to be affected by a specific actin isovariant ACT7. Intracellular PIN1 and PIN2 protein agglomerations were observed in *act7* and *act7act8* mutants but not in *act2*, *act8* or *act2act8* mutants (Figs. 3 and 4). Further, the PIN2 protein aggregation was observed only in the meristem cells of *act7* and *act7act8*, not in the cells of transition zone (Fig. 4). For PIN7, loss of ACT7 results in a slight reduction in the expression of the protein, which is further downregulated in *act7act8* double mutant. No notable change in PIN7 expression was observed in *act8* or *act2act8* mutant background (Fig. 5). On the other hand, loss of ACT7 or ACT8 does not affect the trafficking or expression of PIN4 or auxin influx carrier AUX1 (Fig. 5).

Taken together, these results suggest that actin isovariant ACT7 provides the primary track for the intracellular trafficking of PIN1 and PIN2 and ACT8 possibly functions as secondary track.

Auxin gradient at root tip is altered in *act7* and *act7act8* mutants

Since the intracellular trafficking of the auxin proteins play important roles in determining the cellular auxin flow and formation of auxin gradients required for maintenance of stem cell niche and meristem development, we next investigated whether the observed alterations of intracellular trafficking of PIN1 and PIN2 affects the auxin gradient formation in actin isovariant mutants. Auxin gradient formation assessment using two widely used auxin reporter lines *DR5-GUS* and *IAA2-GUS* revealed that actin isovariant ACT7 plays a major role in regulating this process as reduced GUS signal was observed at the *act7* root tip (Fig. 6). Auxin gradient formation was not altered in *act8* mutant. *act7act8* double mutant shows a complete loss of auxin gradient at the root tip, although the GUS signal could be observed in the upper part of the root (Fig. 6). Exogenous application of IAA could increase the GUS signal at the root tip of *act7* but not in *act7act8* (Fig. 6). These results confirm that the root auxin gradient formation is primarily dependent on actin isovariant ACT7 regulated PIN1 and PIN2-mediated auxin flow.

Auxin transport is altered in *act7* mutant

To confirm that the reduced auxin gradient in *act7* mutant is due to reduced transport resulting from the altered trafficking of PIN1 and PIN2, we performed the auxin transport assay using radiolabeled IAA. Compared with wild-type, both rootward and shootward transports were found to be reduced in *act7-4* mutant, confirming that the observed reduction in auxin gradient at root tip is due to the altered transport of auxin (Fig. 7).

Ethylene response is altered in *act7* and *act7act8* mutants

Auxin and ethylene function as collaborators for primary root development (Muday et al., 2012), and it has been shown that reduction in intracellular auxin level affects the cellular ethylene response (Rahman et al., 2001; Rahman et al., 2002; Stepanova et al., 2005; Stepanova et al., 2007; Swarup et al., 2007). Since ethylene is involved in regulating stem cell niche (Ortega-Martínez et al., 2007) and directly influences the root meristem cell division, we checked whether the reduced meristematic cell division observed in *act7* and *act7act8* mutants are also linked to root ethylene response. To clarify the issue, first we investigated whether the ethylene-induced auxin response is altered. For this, we investigated the expression of a reporter line containing transcriptional fusion of *ANTHRANILATE SYNTHASE β1* to *GUS* (*ASB1-GUS*), which catalyzes one of the rate-limiting steps of tryptophan biosynthesis, a precursor of IAA (Stepanova et al., 2005), and is

specifically induced by ethylene (Guo and Ecker, 2004; Stepanova et al., 2005; Okamoto et al., 2008). Consistent with the previous report, in the wild type, the GUS activity driven by *ASB1* was found to be exclusively localized in the root tip, and no expression in the elongation zone (Stepanova et al., 2005; Figure 8A). Loss of ACT7 and both ACT7 and ACT8 result in ectopic GUS expression. In *act7* and *act7act8* mutants, although complete loss of GUS activity was observed at the root tip, unusual high activity was observed in the elongation zone, suggesting that ethylene-induced auxin production at root tip is blocked in these mutant backgrounds (Fig. 8A). To further understand whether the reduction in auxin response also affects the ethylene response, we investigated the expression of the *ETR2, CTR1* and *EIN2*, that regulate the ethylene response pathway. Although *ETR2* and *CTR1*expression was unaltered in *act7* and *act7act8* mutants, *EIN2*, which functions as a positive regulator for ethylene response (Alonso, 1999) was found to be down regulated in both the mutant backgrounds (Fig. 8 B-D). The down regulation of *ASB1*, and *EIN2* suggest that along with auxin, ethylene response is also affected by loss of ACT7 and ACT8, and ACT7 plays a primary role in this process.

Altered meristem development of *act7* and *act7act8* mutants is independent of cytokinin

Auxin-cytokinin interaction is another major regulator of root meristem development (Dello Ioio et al., 2007). Since *act7* and *act7act8* mutants showed a clear defect in meristematic cell production rate and showed altered response to auxin, we next investigated whether the cytokinin response is also affected by the loss of actin isovariants. For this, we observed the expression of cytokinin specific synthetic marker TCS-GFP, and analyzed the cytokinin specific genes *ARR1, ARR12* (Muller and Sheen, 2007) expression in *act7* and *act7act8* mutant backgrounds. Unlike auxin markers, we did not observe any alteration in the expression of cytokinin responsive marker or genes in *act7* and *act7act8* mutant backgrounds (Fig.9). Interestingly, expression of *Aux/IAA* gene *SHY2*/*IAA3* (Tian and Reed, 1999) was found to be drastically reduced in both *act7* and *act7act8* mutants. Taken together, these results suggest that the altered meristem development in *act7* and *act7act8* mutants is regulated through a pathway that is independent of cytokinin response.

Discussion

Root organogenesis largely relies on the primary root meristem development, which in turn is regulated by the coordinated function of cell division, cell differentiation and cell elongation. Plant hormones auxin, cytokinin and ethylene have been shown to control this coordination and local auxin gradient formed by the polar transport of auxin turns out to be the regulatory switch in integrating all these aspects. Earlier, it was shown that cytokinin promotes root cell differentiation through suppressing the auxin distribution in the meristem (Dello Ioio et al., 2008a; Růzičkа et al., 2009), and formation of local auxin gradient at the root apex promotes the cell division (Brumos et al., 2018). Ethylene also affects the root development through modulating auxin transport and auxin gradient (Růzicka et al., 2007; Lewis et al., 2011). The formation of auxin gradient depends on the polar transport of auxin, which is regulated by the intracellular trafficking mediated correct localization of the cellular auxin efflux carriers PINs (Luschnig et al., 1998; Geldner et al., 2001). The cell cytoskeleton component actin plays a major role in facilitating the trafficking of auxin efflux carriers by providing track for the movement of these proteins (Geldner et al., 2001; Muday and Murphy, 2002; Rahman et al., 2007; Kleine-Vehn et al., 2008). However, what remains obscure is which type of actin contributes to this trafficking process and whether they directly regulate the cellular auxin gradient formation and thereby root meristem development. Taking advantage of the vegetative class actin isovariant mutants, in this study we answered these questions. Our results demonstrate that root meristem maintenance is largely dependent on the ACT7 class actin filament but not on ACT8 and ACT2 (Fig. 2). Loss of ACT7 results in fragmented and depolymerized actin that affects the expression and trafficking of a subset of auxin efflux carriers mainly PIN1, PIN2 and PIN7 and subsequently the polar transport mediated auxin gradient at the root tip (Figs. 1, 3, 4, 5, 6). The consequence of this cascade results in reduced cell division and shorter root meristem (Fig. 2). These findings are consistent with the previous results showing that disruption of actin, by actin depolymerization drug Latranculin B resulted in reduced cell division and inhibition of primary root elongation (Baluška et al., 2001; Rahman et al., 2007), and *act7* mutant shows a dwarf seedling phenotype including a severe reduction in the primary root elongation (Gilliland et al., 2003). The actin structure, trafficking and expression of PIN proteins and root meristem development were completely unaffected in absence of other vegetative class actin isovariants ACT2 or ACT8. Collectively, these results suggest that intact actin cytoskeleton maintained by ACT7 isovariant is the primary regulator of root meristem development.

The analysis of the actin isovariant mutants clearly supported the previous claims that the trafficking of the auxin efflux carriers PIN1 and PIN2 is actin dependent (Geldner et al., 2001; Muday and Murphy, 2002; Rahman et al., 2007). It further clarifies that ACT7 isovariant is the main regulatory actin for this process as PIN1 and PIN2 trafficking as well as the auxin gradient at the tip are not affected at all by the loss of ACT2 and ACT8 (Figs. 3, 4, 6). Interestingly, PIN4, PIN7 and AUX1 trafficking is not affected by the loss of ACT7, suggesting that not all auxin carriers trafficking is actin dependent (Fig. 5). The ACT7 mediated PIN1 and PIN2 trafficking is possibly regulated by the ABCB chaperone TWISTED DWARF1 (TWD1) as ACT7 was found to be an indirect interactor of TWD1 (Zhu et al., 2016). However, there could be other ACT7 interacting proteins that may regulate this process and need to be identified. The finding that only one actin isovariant ACT7 affects the root meristem developmental process through modulating auxin distribution is not inconsistent as it was previously shown that ACT7 affects the primary root growth and response to auxin during callus formation (Kandasamy et al., 2001; Kandasamy et al., 2009).

The reduced meristem growth in *act7* was found to be linked to the inhibition of cell division and cell elongation (Fig. 2, Table 1). Our results suggest that this growth reduction and the inhibition of cell division are directly linked to the auxin maximum at the root tip. In *act7* mutant, we observed a depletion in auxin maximum, while in *act7act8* mutant the auxin maximum was absent at the root tip (Fig. 6). The reduced auxin maximum in *act7* and *act7act8* mutant is a consequence of both reduction in polar transport of auxin, and the auxin synthesis at root tip (Figs. 7 and 8). This difference in auxin maximum is reflected in their root meristem development and cell division where *act7act8* shows more severe phenotype compared with *act7* (Fig. 2; Table 1). Interestingly, although these mutants show less or no auxin maxima at root tip, they showed auxin response in elongation zone confirming that they retain the capability to respond to auxin. Consistently, exogenous application of auxin results in increased response in the elongation zone (Fig. 6). These results are consistent with the idea that local auxin maximum at root tip is an absolute requirement for meristematic cell division and meristem growth (Grieneisen et al., 2007; Brumos et al., 2018).

The reduction in the intracellular auxin level at the root meristem also affected the ethylene response. Ethylene specific auxin biosynthesis gene *ASβ1*, and the central ethylene response regulator *EIN2* were down regulated in the root meristem of both *act7* and *act7act8* mutants (Fig.

8). This is consistent with the previous findings that intracellular auxin level regulates the root ethylene response, and the response can be restored by alleviating the intracellular auxin level (Rahman et al., 2001; Muday and Murphy, 2002; Rahman et al., 2002). Collectively, these results suggest that the altered root meristem development in *act7* and *act7act8* mutants is a consequence of loss of both auxin and ethylene responses.

Involvement of auxin-cytokinin interaction in root meristem development has been well studied and shown to be controlled through a balance between cell division and cell differentiation mediated by a simple regulatory circuit converging on Aux/IAA family protein SHY2/IAA3 (Dello Ioio et al., 2008a; Moubayidin et al., 2010). The primary cytokinin- response transcription factors *ARR1* and *ARR12* activates the *SHY2/IAA3*, a repressor of auxin signaling, that negatively regulates the expression of *PIN1*, *PIN3* and *PIN7* genes and thereby alters the auxin distribution in the root meristem (Dello Ioio et al., 2008a; Růžička et al., 2009; Moubayidin et al., 2010). To understand whether the altered auxin maximum at the root tip and the altered root meristem development of *act7 a*nd *act8* is a consequence of altered cytokinin response, we investigated the expression of *ARR1*, *ARR12* and *SHY2/IAA3* in the mutant background. Neither *ARR1*, nor *ARR12* expression was altered in *act7* or *act7act8* double mutant. Consistently, we also did not observe any change in the synthetic cytokinin marker *TCS-GFP* (Fig. 9). Interestingly, we found that *SHY2/IAA3*, which belong to primary auxin responsive gene family *Aux/IAA* (Abel and Theologis, 1996) was downregulated in both *act7* and *act7act8* mutants (Fig. 9). *IAA3* has also been shown to directly influence the auxin-regulated Arabidopsis root development (Tian and Reed, 1999). These observations confirm that the altered root meristem development observed in loss of ACT7 mutant is directly linked to altered auxin response. *ARR1*, *ARR12* regulated *SHY2*/*IAA3*pathway is more dominant in older seedlings compared with younger seedlings as at the early seedling stage only *ARR12* is expressed and *SHY2* level is relatively low (Moubayidin et al., 2010). Consistently, auxin regulated cell division predominates over cytokinin regulated cell differentiation to shape the meristem development at early seedling stage (Chapman and Estelle, 2009; Moubayidin et al., 2010). The observation that the altered root meristem development in the loss of ACT7 is primarily dependent on auxin response and independent of cytokinin is consistent with above findings as we characterized the root meristem at the early stage of development.

In conclusion, in the present study we demonstrated that primary root meristem development is exclusively controlled by actin isovariant ACT7 mediated auxin redistribution in the root tip and primarily regulated by auxin-ethylene interaction but independent of cytokinin.

Materials and methods

Plant materials and growth conditions

All lines are in the Columbia background of *Arabidopsis thaliana* (L.). *ASB1-GUS* was a gift of Jose Alonso (University of North Carolina, Raleigh, USA), PIN2-GFP (Xu and Scheres, 2005) was gift of B. Scherers (University of Utrecht, The Netherlands), GFP-ABD2–GFP (Wang et al., 2007) was a gift of E.B. Blancaflor (Samuel Roberts Noble Foundation, Ardmore, OK, USA). *IAA2:GUS* and AUX1-YFP were gifts of Malcolm Bennett (Swarup et al., 2007). PIN4-GFP and PIN7-GFP were gift of Gloria Muday (Wake Forest University, NC, USA). Columbia-0, PIN1-GFP and *aux1-7* were obtained from the Arabidopsis Biological Resource Center (Columbus, OH, USA). The *act8-2, act7-4* a*ct7act8, act2-1,* and *act2act8* were gifts of R. Meagher (University of Georgia, Athens, Georgia). Various marker lines in actin isovariant mutant background were generated in the laboratory by crossing, and independent homozygous lines for the mutation and expressing the GFP or GUS reporter were identified by screening for fluorescence, GUS assay and seedling phenotype.

Seeds were sterilized in 20% kitchen bleach (Coop Clean Co., http://www.coopclean.co.jp) for 15 minutes and washed 3 times in sterilized dH_2O. Surface-sterilized seeds were placed in round, 9 cm Petri plates on modified Hoagland' s medium (Baskin and Wilson, 1997) containing 1% w/v sucrose and 1% w/v ager (Difco Bacto ager, BD laboratories; http://www.bd.com). Two days after stratification at 4°C in the dark, plates were transferred to growth chamber (NK system, LH-70CCFL-CT, Japan, http://www.nksystems.co.jp/) at 23°C under continuous white light at an irradiance of about 100 µmol m^{-2} s^{-1}. The seedlings were grown vertically for 5 or 7 days.

Chemicals

IAA was purchased from Sigma-Aldrich Chemical Company (http://www.sigmaaldrich.com). Other chemicals were purchased from Wako Pure Chemical Industries (http://www.wako-chem.co.jp/). FM4-64 was purchased from Invitogen

(http://www.thermofisher.com). [^{3}H] IAA (20 Ci mmol^{-1}) was purchased from American Radiolabeled Chemicals (http://www.arcinusa.com).

Growth, cell length and cell production rate assays

Root elongation rate was measured by scoring the position of the root tip on the back of the Petri plate once per day. Cortical cell length was measured using light microscope (Diaphot, Nikon, www.nikon.co.jp) equipped with a digital camera control unit (Digital Sight [DS-L2], Nikon) as described earlier (Rahman et al., 2007). To ensure newly matured cells were scored, no cell was measured closer to the tip than the position where root hair length was roughly half maximal. The length of 20 mature cortical cells was measured from each root, with eight roots used per treatment. The cell production rate (cells day^{-1}) was calculated by taking the ratio of root elongation rate (mm day^{-1}) and average cell length (μm) for each individual and averaging over all the roots in the treatment. The results were obtained from at least three biological replicates per genotype.

GUS staining, immunostaining, and live cell imaging

GUS staining was performed as described earlier (Okamoto et al., 2008). In brief, 5-d-old vertically grown seedlings were used for GUS assay. Seedlings were transferred to GUS staining buffer (100 mM sodium phosphate pH 7.0, 10 mM EDTA, 0.5 mM potassium ferricyanide, 0.5 mM potassium ferrocyanide, and 0.1 % Triton X-100) containing 1mM X-gluc and incubated at 37°C in the dark for various time length as mentioned in the figure legends. To observe the effect of exogenous auxin on GUS expression, the seedlings were incubated in 1 μM IAA for 3h and subjected to GUS staining as described above. Roots were cleared as described earlier (Shibasaki et al., 2009). The roots were imaged with a light microscope (Nikon Diaphot) equipped with a digital camera control unit (Digital sight, DS-L2; Nikon).

Actin immunostaining was performed using the protocol described earlier by Rahman et al. (2007) with modification. In brief, Five-day-old Arabidopsis seedlings were fixed in PIPES buffer (50 mM PIPES, 4% paraformaldehyde, 1.2% glutaraldehyde, 1 mM CaCl2, 0.4 mM maleimidobenzoyl-N-hydroxy succinimide) for 60 min, followed by rinsing in PME buffer (50 mM PIPES, 5 mM EGTA, and 2 mM MgSO4) 3 times for 10 min each. After the PME washing, the seedlings were extracted for 60 min in PME buffer containing 1% Triton X-100. The seedlings

were then subjected to digestion for 15 min in PBS with 0.001% pectolyase and 0.01% pectinase, and rinsed three times for 5 min in PME with 10% glycerol and 0.002% Triton X-100. Seedlings were permeabilized by incubating them at −20°C in methanol for 30 min, followed by rehydration in PBS for three times 5 min each. Seedlings were incubated in the primary mouse monoclonal anti-(chicken gizzard) actin, clone 4 (Millipore, http://www.millipore.com) diluted 1:200 in PBS, 1% BSA, and 0.01% sodium azide (PBA) overnight. After the incubation, the seedlings were washed for three times 5 min each and then incubated in the secondary antibody Cy-3-goat anti-mouse IgG (1:200; Jackson Immunoresearch, http://www.jacksonimmuno.com). The imaging was performed on a Nikon laser scanning microscope (Eclipse Ti equipped with Nikon C2 Si laser scanning unit) equipped with a ×60 oil immersion objective.

To image GFP, YFP and FM 4-64-stained roots, five-day-old seedlings were mounted in liquid growth medium on a cover glass for observation on a Nikon laser scanning microscope (Eclipse Ti equipped with Nikon C2 Si laser scanning unit) and imaged with either a ×20 dry or ×40 water immersion objectives. The images were taken using the same confocal settings for each set of experiments. All the experiments were repeated at least 3 times.

Auxin transport assay

Five-day-old vertically grown *Arabidopsis* seedlings were used for auxin transport assay. Auxin transport was measured as described earlier (Shibasaki et al., 2009). In brief, a donor drop was prepared by mixing 0.5 μM [^{3}H] IAA (3.7 MBq ml^{-1}) in 1.5% agar containing MES buffer solution. The donor drop was placed on the edge of the root tip for the shootward auxin transport assay or at the root-shoot junction for the rootward transport assay. Plates were then incubated vertically at 23°C for 2h for shootward auxin transport assay and 6h for rootward auxin transport assay. For measurement of auxin transport, 5-mm root segments away from the apical 2 mm root tip and 2 mm away from the root-shoot junction were carefully cut and soaked overnight in 4 ml of liquid scintillation fluid (Ultima Gold, PerkinElmer, USA), and the radioactivity was measured with a scintillation counter (model LS6500, Beckman ACSII; USA Instruments, Fullerton, CA). Data were obtained from at least three biological replicates.

Gene expression analysis

RNA was extracted from 5-day-old vertically grown *Arabidopsis thaliana* seedlings root tissue using RNeasy Mini Kit (Qiagen, www.qiagen.com) with on-column DNA digestion to remove residual genomic DNA using RNase-free DNase according to manufacturer's protocol. Extracted RNA was tested for quality and quantity. Each RNA concentration was normalized with RNase free water. 500 ng RNA was used to synthesize cDNA using Rever Tra Ace qPCR RT master mix (Toyobo, Japan, www.toyobo-global.com). Quantitative PCR reactions were performed using the Takara TP-850 thermal cycler (Takara Bio, Japan, www.takara-bio.com) and THUNDERBIRDTM SYBR® qPCR Mix from Toyobo (https://www.toyobo.co.jp). The reaction was performed as per manufacturer's instruction. For quantification of gene expression, we used the $2^{-\Delta\Delta}$CT (cycle threshold) method (Livak and Schmittgen, 2001) with a normalization to the *ef1α* expression. Data were obtained from three biological replicates. Primers used for the gene expression analysis are listed in Supplemental Table 1.

Statistical analysis

Results are expressed as the means ± SE from the appropriate number of experiments. A two-tailed Student's *t*-test was used to analyze statistical significance.

Acknowledgements

The authors thank Jose Alonso (University of North Carolina, Raleigh, USA), B. Scherers (University of Utrecht, The Netherlands), E.B. Blancaflor (Samuel Roberts Noble Foundation, Ardmore, OK, USA), Malcolm Bennett (University of Nottingham, UK). This work was funded by JSPS Kakenhi (Grant Number 23012003 A.R.). We thank Michiko Saito for technical assistance.

Author Contribution

A.R., A.A.R. designed the experiments. T.N. and K.S. performed the plant experiments and cloning of the genes. A.R. supervised the experiments. A.R., T.N., and K.S. analyzed the data. A.R. and A.A.R. wrote the manuscript.

References

Abel S, Theologis A (1996) Early genes and auxin action. Plant Physiol **111**: 9–17

508 **Alonso JM** (1999) EIN2, a Bifunctional Transducer of Ethylene and Stress Responses in
509 Arabidopsis. Science (80) **284**: 2148–2152

510 **Baluška F, Jasik J, Edelmann HG, Salajová T, Volkmann D** (2001) Latrunculin B-Induced
511 Plant Dwarfism: Plant Cell Elongation Is F-Actin-Dependent. Dev Biol **231**: 113–124

512 **Barton MK** (2010) Twenty years on: The inner workings of the shoot apical meristem, a
513 developmental dynamo. Dev Biol **341**: 95–113

514 **Baskin TI, Wilson JE** (1997) Inhibitors of Protein Kinases and Phosphatases Alter Root
515 Morphology and Disorganize Cortical Microtubules. Plant Physiol **113**: 493–502

516 **Beemster GTS, Baskin TI** (1998) Analysis of Cell Division and Elongation Underlying the
517 Developmental Acceleration of Root Growth in Arabidopsis thaliana. Plant Physiol **116**:
518 1515–1526

519 **Benková E, Michniewicz M, Sauer M, Teichmann T, Seifertová D, Jürgens G, Friml J**
520 (2003) Local, Efflux-Dependent Auxin Gradients as a Common Module for Plant Organ
521 Formation. Cell **115**: 591–602

522 **Bertell G, Eliasson L** (1992) Cytokinin effects on root growth and possible interactions with
523 ethylene and indole-3-acetic acid. Physiol Plant **84**: 255–261

524 **Brumos J, Robles LM, Yun J, Vu TC, Jackson S, Alonso JM, Stepanova AN** (2018) Local
525 Auxin Biosynthesis Is a Key Regulator of Plant Development. Dev Cell **47**: 306-318.e5

526 **Chapman EJ, Estelle M** (2009) Cytokinin and auxin intersection in root meristems. Genome
527 Biol **10**: 210

528 **Clayton L, Lloyd CW** (1985) Actin organization during the cell cycle in meristematic plant
529 cells. Exp Cell Res **156**: 231–238

530 **Dello Ioio R, Linhares FS, Sabatini S** (2008a) Emerging role of cytokinin as a regulator of
531 cellular differentiation. Curr Opin Plant Biol **11**: 23–27

532 **Dello Ioio R, Linhares FS, Scacchi E, Casamitjana-Martinez E, Heidstra R, Costantino P,**
533 **Sabatini S** (2007) Cytokinins Determine Arabidopsis Root-Meristem Size by Controlling

534 Cell Differentiation. Curr Biol **17**: 678–682

535 **Dello Ioio R, Nakamura K, Moubayidin L, Perilli S, Taniguchi M, Morita MT, Aoyama T,**
536 **Costantino P, Sabatini S** (2008b) A genetic framework for the control of cell division and
537 differentiation in the root meristem. Science (80-) **322**: 1380–1384

538 **Feraru E, Friml J** (2008) PIN Polar Targeting. Plant Physiol **147**: 1553–1559

539 **Friml J** (2003) Auxin transport — shaping the plant. Curr Opin Plant Biol **6**: 7–12

540 **Geldner N, Friml J, Stierhof Y-D, Jürgens G, Palme K** (2001) Auxin transport inhibitors
541 block PIN1 cycling and vesicle trafficking. Nature **413**: 425–428

542 **Gilliland LU, Kandasamy MK, Pawloski LC, Meagher RB** (2002) Both vegetative and
543 reproductive actin isovariants complement the stunted root hair phenotype of the
544 Arabidopsis act2-1 mutation. Plant Physiol **130**: 2199–2209

545 **Gilliland LU, Pawloski LC, Kandasamy MK, Meagher RB** (2003) Arabidopsis actin gene
546 ACT7 plays an essential role in germination and root growth. Plant J **33**: 319–328

547 **Grieneisen VA, Xu J, Marée AFM, Hogeweg P, Scheres B** (2007) Auxin transport is sufficient
548 to generate a maximum and gradient guiding root growth. Nature **449**: 1008–1013

549 **Guo H, Ecker JR** (2004) The ethylene signaling pathway: new insights. Curr Opin Plant Biol **7**:
550 40–49

551 **Huang J-D, Brady ST, Richards BW, Stenoien D, Resau JH, Copeland NG, Jenkins NA**
552 (1999) Direct interaction of microtubule- and actin-based transport motors. Nature **397**:
553 267–270

554 **Kandasamy MK, Burgos-Rivera B, McKinney EC, Ruzicka DR, Meagher RB** (2007) Class-
555 specific interaction of profilin and ADF isovariants with actin in the regulation of plant
556 development. Plant Cell **19**: 3111–3126

557 **Kandasamy MK, Gilliland LU, McKinney EC, Meagher RB** (2001) One plant actin
558 isovariant, ACT7, is induced by auxin and required for normal callus formation. Plant Cell
559 **13**: 1541–1554

Kandasamy MK, McKinney EC, Meagher RB (2009) A single vegetative actin isovariant overexpressed under the control of multiple regulatory sequences is sufficient for normal Arabidopsis development. Plant Cell **21**: 701–18

Kim H, Park M, Soo JK, Hwang I (2005) Actin filaments play a critical role in vacuolar trafficking at the Golgi complex in plant cells. Plant Cell **17**: 888–902

Kleine-Vehn J, Friml J (2008) Polar Targeting and Endocytic Recycling in Auxin-Dependent Plant Development. Annu Rev Cell Dev Biol **24**: 447–473

Kleine-Vehn J, Leitner J, Zwiewka M, Sauer M, Abas L, Luschnig C, Friml J (2008) Differential degradation of PIN2 auxin efflux carrier by retromer-dependent vacuolar targeting. Proc Natl Acad Sci U S A **105**: 17812–17817

Lewis DR, Negi S, Sukumar P, Muday GK (2011) Ethylene inhibits lateral root development, increases IAA transport and expression of PIN3 and PIN7 auxin efflux carriers. Development **138**: 3485–3495

Liu Y, Xu M, Liang N, Zheng Y, Yu Q, Wu S (2017) Symplastic communication spatially directs local auxin biosynthesis to maintain root stem cell niche in Arabidopsis. Proc Natl Acad Sci U S A **114**: 4005–4010

Livak KJ, Schmittgen TD (2001) Analysis of Relative Gene Expression Data Using Real-Time Quantitative PCR and the 2−ΔΔCT Method. Methods **25**: 402–408

Lloyd CW (1991) How does the cytoskeleton read the laws of geometry in aligning the division plane of plant cells? Development **112**: 55–65

Luschnig C, Gaxiola RA, Grisafi P, Fink GR (1998) EIR1, a root-specific protein involved in auxin transport, is required for gravitropism in Arabidopsis thaliana. Genes Dev **12**: 2175–2187

McDowell JM, An YQ, Huang S, McKinney EC, Meagher RB (1996) The arabidopsis ACT7 actin gene is expressed in rapidly developing tissues and responds to several external stimuli. Plant Physiol **111**: 699–711

586 **McLean BG, Huang S, McKinney EC, Meagher RB** (1990) Plants contain highly divergent
587 actin isovariants. Cell Motil Cytoskeleton **17**: 276–290

588 **Meagher RB** (1991) Divergence and Differential Expression of Actin Gene Families in Higher
589 Plants. Int Rev Cytol **125**: 139–163

590 **Moubayidin L, Perilli S, Dello Ioio R, Di Mambro R, Costantino P, Sabatini S** (2010) The
591 rate of cell differentiation controls the arabidopsis root meristem growth phase. Curr Biol
592 **20**: 1138–1143

593 **Muday GK, Murphy AS** (2002) An emerging model of auxin transport regulation. Plant Cell
594 **14**: 293–299

595 **Muday GK, Rahman A, Binder BM** (2012) Auxin and ethylene: Collaborators or competitors?
596 Trends Plant Sci **17**: 181–195

597 **Muller B, Sheen J** (2007) Arabidopsis Cytokinin Signaling Pathway. Sci STKE **2007**: 1–5

598 **Müller B, Sheen J** (2007) Arabidopsis cytokinin signaling pathway. Sci STKE **2007**: 1–5

599 **Nebenführ A, Staehelin LA** (2001) Mobile factories: Golgi dynamics in plant cells. Trends
600 Plant Sci **6**: 160–167

601 **Nishimura T, Yokota E, Wada T, Shimmen T, Okada K** (2003) An Arabidopsis ACT2
602 Dominant-Negative Mutation, which Disturbs F-actin Polymerization, Reveals its
603 Distinctive Function in Root Development. Plant Cell Physiol **44**: 1131–1140

604 **Okamoto T, Tsurumi S, Shibasaki K, Obana Y, Takaji H, Oono Y, Rahman A** (2008)
605 Genetic dissection of hormonal responses in the roots of Arabidopsis grown under
606 continuous mechanical impedance. Plant Physiol **146**: 1651–1662

607 **Ortega-Martínez O, Pernas M, Carol RJ, Dolan L** (2007) Ethylene modulates stem cell
608 division in the Arabidopsis thaliana root. Science **317**: 507–10

609 **Pollard TD, Cooper JA** (2009) Actin, a central player in cell shape and movement. Science
610 (80-) **326**: 1208–1212

611 **Rahman A** (2013) Auxin: A regulator of cold stress response. Physiol Plant **147**: 28–35

612 **Rahman A, Amakawa T, Goto N, Tsurumi S** (2001) Auxin is a positive regulator for ethylene-
613 mediated response in the growth of arabidopsis roots. Plant Cell Physiol **42**: 301–307

614 **Rahman A, Bannigan A, Sulaman W, Pechter P, Blancaflor EB, Baskin TI** (2007) Auxin,
615 actin and growth of the Arabidopsis thaliana primary root. Plant J **50**: 514–528

616 **Rahman A, Hosokawa S, Oono Y, Amakawa T, Goto N, Tsurumi S** (2002) Auxin and
617 ethylene response interactions during Arabidopsis root hair development dissected by auxin
618 influx modulators. Plant Physiol **130**: 1908–1917

619 **Ringli C, Baumberger N, Diet A, Frey B, Keller B** (2002) ACTIN2 is essential for bulge site
620 selection and tip growth during root hair development of arabidopsis. Plant Physiol **129**:
621 1464–1472

622 **Růzicka K, Ljung K, Vanneste S, Podhorská R, Beeckman T, Friml J, Benková E** (2007)
623 Ethylene regulates root growth through effects on auxin biosynthesis and transport-
624 dependent auxin distribution. Plant Cell **19**: 2197–2212

625 **Růzička K, Šimášková M, Duclercq J, Petrášek J, Zažímalová E, Simon S, Friml J, Van**
626 **Montagu MCE, Benková E** (2009) Cytokinin regulates root meristem activity via
627 modulation of the polar auxin transport. Proc Natl Acad Sci U S A **106**: 4284–4289

628 **Shibasaki K, Uemura M, Tsurumi S, Rahman A** (2009) Auxin response in Arabidopsis under
629 cold stress: underlying molecular mechanisms. Plant Cell **21**: 3823–3838

630 **Silk WK, Lord EM, Eckard KJ** (1989) Growth Patterns Inferred from Anatomical Records.
631 Plant Physiol **90**: 708–713

632 **Simon VR, Pon LA** (1996) Actin-based organelle movement. Experientia **52**: 1117–1122

633 **Smith LG, Oppenheimer DG** (2005) Spatial control of cell expansion by the plant
634 cytoskeleton. Annu Rev Cell Dev Biol **21**: 271–295

635 **Staiger CJ, Blanchoin L** (2006) Actin dynamics: old friends with new stories. Curr Opin Plant
636 Biol **9**: 554–62

637 **Staiger CJ, Schliwa M** (1987) Actin localization and function in higher plants. Protoplasma
638 **141**: 1–12

639 **Stepanova AN, Hoyt JM, Hamilton AA, Alonso JM** (2005) A link between ethylene and auxin
640 uncovered by the characterization of two root-specific ethylene-insensitive mutants in
641 arabidopsis. Plant Cell **17**: 2230–2242

642 **Stepanova AN, Robertson-Hoyt J, Yun J, Benavente LM, Xie DY, Doležal K, Schlereth A,**
643 **Jürgens G, Alonso JM** (2008) TAA1-Mediated Auxin Biosynthesis Is Essential for
644 Hormone Crosstalk and Plant Development. Cell **133**: 177–191

645 **Stepanova AN, Yun J, Likhacheva A V, Alonso JM** (2007) Multilevel interactions between
646 ethylene and auxin in Arabidopsis roots. Plant Cell **19**: 2169–2185

647 **Street IH, Aman S, Zubo Y, Ramzan A, Wang X, Shakeel SN, Kieber JJ, Eric Schaller G**
648 (2015) Ethylene inhibits cell proliferation of the arabidopsis root meristem. Plant Physiol
649 **169**: 338–350

650 **Swarup R, Perry P, Hagenbeek D, Van Der Straeten D, Beemster GTS, Sandberg G,**
651 **Bhalerao R, Ljung K, Bennett MJ** (2007) Ethylene upregulates auxin biosynthesis in
652 Arabidopsis seedlings to enhance inhibition of root cell elongation. Plant Cell **19**: 2186–
653 2196

654 **Tian Q, Reed JW** (1999) Control of auxin-regulated root development by the Arabidopsis
655 thaliana SHY2/IAA3 gene. Development **126**: 711–21

656 **Vaškebová L, Šamaj J, Ovecka M** (2018) Single-point ACT2 gene mutation in the Arabidopsis
657 root hair mutant der1-3 affects overall actin organization, root growth and plant
658 development. Ann Bot **122**: 889–901

659 **Wang Y-S, Yoo C-M, Blancaflor EB** (2007) Improved imaging of actin filaments in transgenic
660 Arabidopsis plants expressing a green fluorescent protein fusion to the C- and N-termini of
661 the fimbrin actin-binding domain 2. New Phytol **177**: 071120093824004-???

662 **Xu J, Scheres B** (2005) Dissection of Arabidopsis ADP-RIBOSYLATION FACTOR 1 function
663 in epidermal cell polarity. Plant Cell **17**: 525–536

Zhu J, Bailly A, Zwiewka M, Sovero V, Di Donato M, Ge P, Oehri J, Aryal B, Hao P, Linnert M, et al (2016) TWISTED DWARF1 Mediates the Action of Auxin Transport Inhibitors on Actin Cytoskeleton Dynamics. Plant Cell **28**: 930–948

Figure Legends

Figure 1. Effect of loss of Actin isovariant proteins on intracellular actin organization.
Upper panel (A-F) chemical fixation. Lower panel (G-L) live cell imaging. The images are representative of at least three fixation runs, with 5–7 roots per genotype in each run. Five-day old Arabidopsis roots were fixed (for chemical fixation) or mounted in liquid growth medium on a cover glass (for live cell imaging) and actin was localized using confocal laser microscopy. The images were obtained from the elongation zone of the root and imaged using the same confocal settings for immunostaining and live cell imaging respectively. Images are projections of 10–12 optical sections. Bars=10 μm for upper panel and 20 μm for lower panel.

Figure 2. ACT7 plays an important role in determining primary root development and meristem size.

(A) Seven-day old seedling phenotype of actin single and double mutants. Loss of ACT7 drastically affects the seedling phenotype, including primary root growth. (B-C) Image and the size of the primary root meristem in actin isovariant mutants. For root meristem imaging, seven-day old seedlings were stained in 2μM FM 4-64 for 15 minute and subjected to imaging using confocal laser microscope using the same settings. Images and data are representative of at least 3-4 biological replicates. Vertical bars represent mean ± SE of the experimental means from obtained from at least 3 experiments (n= 3 or more), where experimental means were obtained from 6-8 seedlings per treatment. Asterisks represent the statistical significance between wild-type and mutants as judged by the Student`s *t*-test (*P<0.5, **P<0.01, ***P< 0.001). Bars, 5 mm (A); 50 μm (B).

Figure 3. Loss of ACT7 but not ACT2 and ACT8 affects the intracellular dynamic cycling of PIN1.
Seven-day old PIN1:PIN1-GFP transgenic seedlings in wild-type and actin single and double mutant background were subjected to confocal imaging. The images were captured using the same confocal settings and are representative of 20 roots from three- four independent experiments. Lower panel represents the zoomed images. The intracellular agglomeration of PIN1, indicated by arrowheads, was observed exclusively in *act7* and *act7act8* mutants. Bars represent 10 μm.

Figure 4. Loss of ACT7 but not ACT2 and ACT8 affects the intracellular dynamic cycling of PIN2.
Seven-day old PIN2:PIN2-GFP transgenic seedlings in wild-type and actin single and double mutant background were subjected to confocal imaging. The images were captured using the same confocal settings and are representative of 25 roots from three- four independent experiments. Upper and middle panel represent the images from the root meristem region. Lower panel represents the images from transition zone. The intracellular agglomeration of PIN2 was observed exclusively in the meristematic region of *act7* and *act7act8* mutants but not in the transition zone (Bottom Panel). Bars represent 10 μm.

Figure 5. Effect of loss of ACT7 on PIN4, PIN7 and AUX1 expression
Seven-day old PIN7:PIN7-GFP, PIN4:PIN4-GFP, and AUX1-YFP transgenic seedlings in wild-type and actin single and double mutant background were subjected to confocal imaging. The images were captured using the same confocal settings and are representative of 20 roots from three- four independent experiments. PIN7 expression was slightly reduced only in *act7act8* mutants. PIN4 and AUX1 expression was unaltered in *act7* and *act7act8* mutants. Bars represent 10 mm. Bars represent 50 μm, and 10 μm for zoomed images of AUX1.

Figure 6. Effect of loss of actin isovariant on the root auxin gradient formation
Five-day old *DR5-GUS* and *IAA2-GUS* transgenic seedlings in wild-type and actin single and double mutant background were subjected to GUS staining. *DR5-GUS* transgenic seedlings were stained in buffer containing 1 mM X- gluc for 3 h and *IAA2-GUS* were stained for 1 h at 37°C. After the incubation, the roots were cleared for photography. Loss of ACT7 results in formation of reduced auxin gradient at root tip. Loss of both ACT7 and ACT8 further enhances the reduction. For exogenous auxin treatment the seedlings were incubated in 1μM IAA for 3h and subjected to GUS staining and cell clearing. The images are representative of 20 seedlings from three-four independent experiments. The results were confirmed with two separate lines for each crossing. Bars represent 100 μm.

Figure 7. Auxin transport is disrupted in *act7* mutant.
Shootward and rootward auxin transport were measured using five-day-old seedlings. The experiments were performed in triplicate and repeated at least three times. Auxin influx facilitator mutant *aux1-7* was used as positive control. Asterisks represent the statistical significance between wild-type and mutants as judged by the Student`s *t*-test (*P<0.5, **P<0.01).

Figure 8. Molecular analysis of ethylene response in *act7* and *act7act8* mutants.
(A) Ectopic expression of ethylene-induced auxin biosynthesis gene *ANTHRANILATE SYNTHASE β1* in the mutants. The expression is reduced at the root tip but stimulated in the elongation zone. The images are representative of 20 seedlings from three independent experiments. Bars represent 50 μm.

(B-D) Expression analysis of the ethylene signaling genes in *act7* and *act7act8* mutants. qRT-PCR was performed using cDNA prepared from the root samples of five-day-old seedlings. All the data were normalized against *ef1α*. The data were obtained from three independent biological replicates. Asterisk represents the statistical significance between wild-type and mutants as judged by the Student`s *t*-test (*P<0.5).

Figure 9. Molecular analysis of cytokinin responsive genes in *act7* and *act7act8* mutants.
(A) Expression analysis of the *ARR1*, *ARR12* and *SHY2/IAA3* in *act7* and *act7act8* mutants. qRT-PCR was performed using cDNA prepared from the root samples of five-day-old seedlings. All the data were normalized against *ef1α*. The data were obtained from three independent biological replicates. Asterisk represents the statistical significance between wild-type and mutants as judged by the Student`s *t*-test (**P<0.01).
(B) Expression of synthetic cytokinin marker *TCS-GFP* is not altered in *act7* and *act7act8* mutants. The images are representative of 20 seedlings from three independent experiments. Bar represents 50 μm.

Table 1: Actin isovariant ACT7 is the primary regulator of root elongation, cell length and cell production in Arabidopsis

Genotype	Primary root elongation (mm)	Cell length (μm)	Cell production rate
Col-0	9.05±0.03	166±1.5	54.0±2.2
act2-1	9.90±0.21	157±0.29*	62.0±0.3*
act7-4	3.39±0.21***	87±5.34***	39.5±2.2***
act8-2	8.90±0.16	166±6.8	52.4±1.3
act2act8	9.09±0.60	159±2.08	61.5±2.3
act7act8	1.8±0.02***	68±7.23***	26.8±2.2***

Data are means ± S.E of three replicate experiments. 4-day-old vertically grown seedlings were transferred to new plates and grown for another three days. The measurements reflect the behavior over the third day of treatment. Asterisks represent the statistical significance between wild-type and mutants as judged by the Student`s *t*-test (*P<0.5, ***P< 0.001).

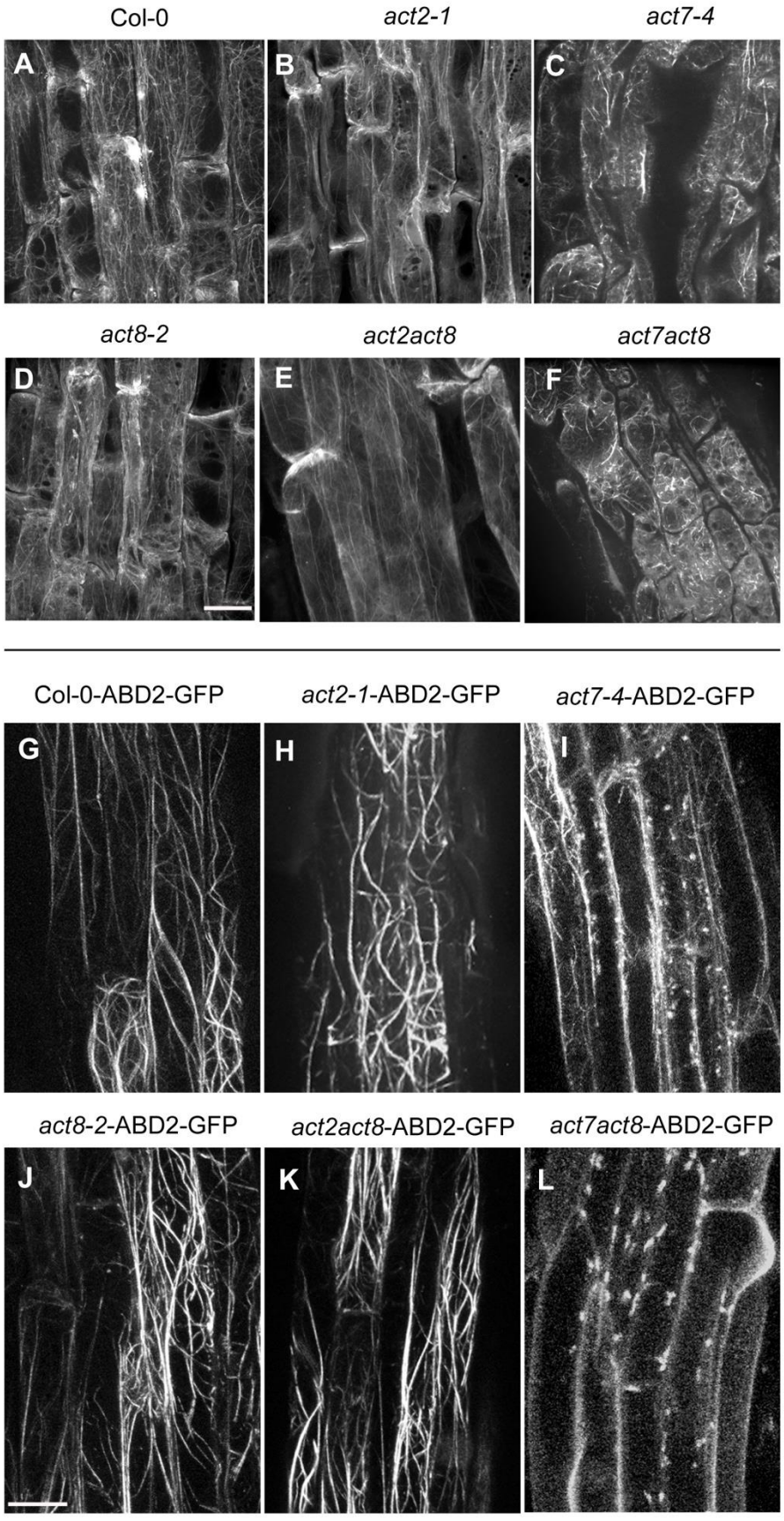

Figure 1.

Effect of loss of Actin isovariant proteins on intracellular actin organization. Upper panel (A-F) chemical fixation. Lower panel (G-L) live cell imaging. The images are representative of at least three fixation runs, with 5–7 roots per genotype in each run. Five-day old Arabidopsis roots were fixed (for chemical fixation) or mounted in liquid growth medium on a cover glass (for live cell imaging) and actin was localized using confocal laser microscopy. The images were obtained from the elongation zone of the root and imaged using the same confocal settings for immunostaining and live cell imaging respectively. Images are projections of 10–12 optical sections. Bars=10 μm for upper panel and 20 μm for lower panel.

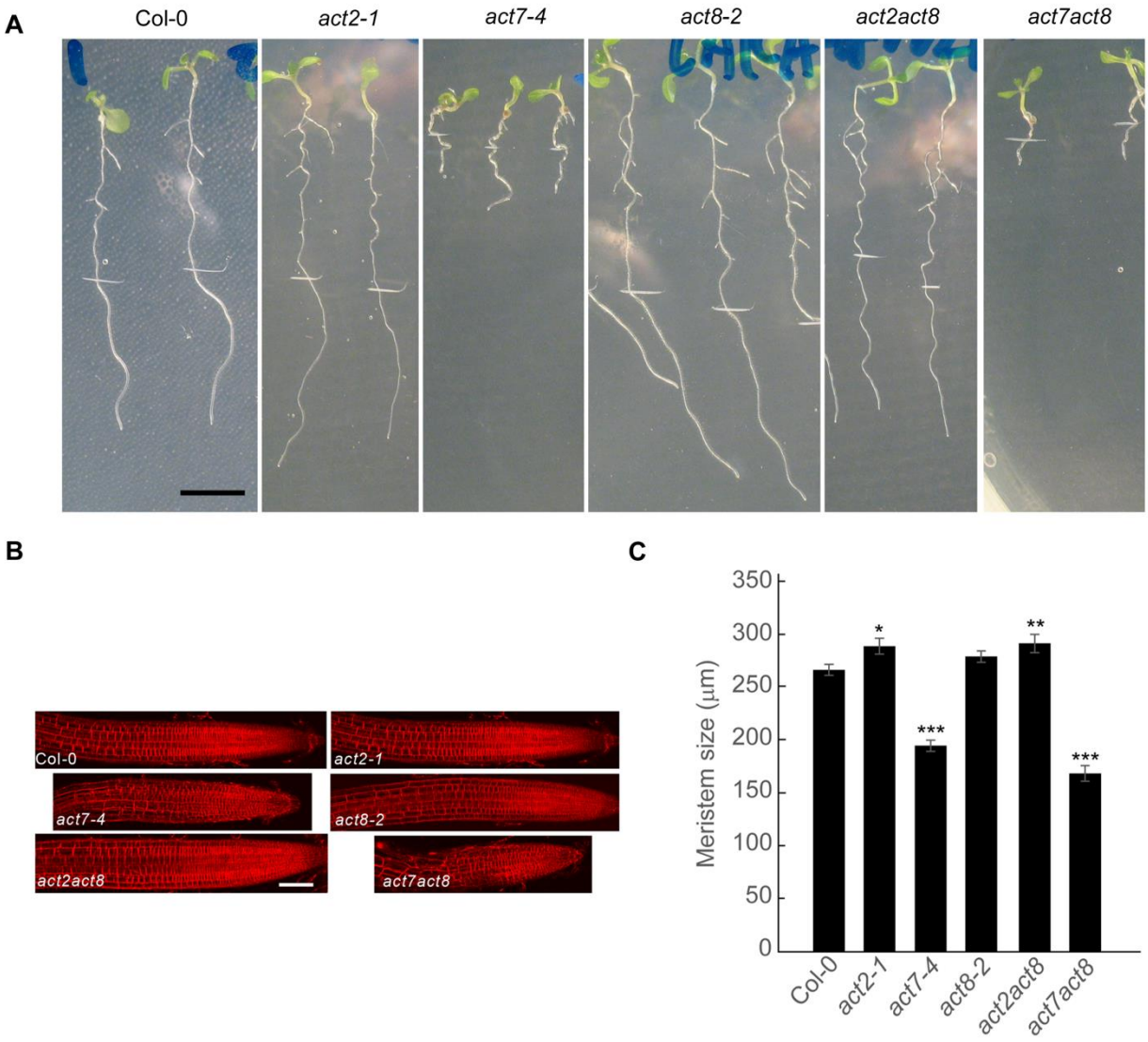

Figure 2. ACT7 plays an important role in determining primary root development and meristem size.

(A) Seven-day old seedling phenotype of actin single and double mutants. Loss of ACT7 drastically affects the seedling phenotype, including primary root growth. (B-C) Image and the size of the primary root meristem in actin isovariant mutants. For root meristem imaging, seven-day old seedlings were stained in 2μM FM 4-64 for 15 minute and subjected to imaging using confocal laser microscope using the same settings. Images and data are representative of at least 3-4 biological replicates. Vertical bars represent mean ± SE of the experimental means from obtained from at least 3 experiments (n=3 or more), where experimental means were obtained from 6-8 seedlings per treatment. Asterisks represent the statistical significance between wild-type and mutants as judged by the Student`s *t*-test (*P<0.5, **P<0.01, ***P< 0.001). Bars, 5 mm (A); 50 μm (B).

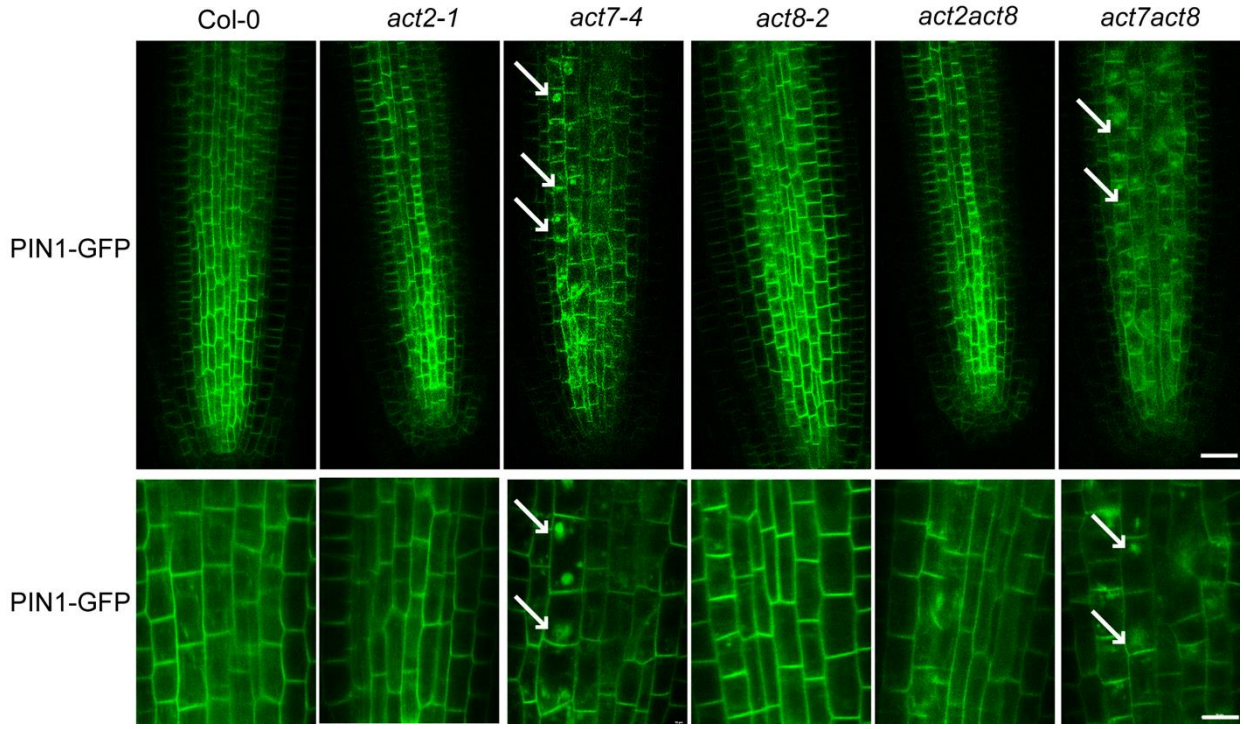

Figure 3. Loss of ACT7 but not ACT2 and ACT8 affects the intracellular dynamic cycling of PIN1.

Seven-day old PIN1:PIN1-GFP transgenic seedlings in wild-type and actin single and double mutant background were subjected to confocal imaging. The images were captured using the same confocal settings and are representative of 20 roots from three- four independent experiments. Lower panel represents the zoomed images. The intracellular agglomeration of PIN1, indicated by arrowheads, was observed exclusively in *act7* and *act7act8* mutants. Bars represent 10 μm.

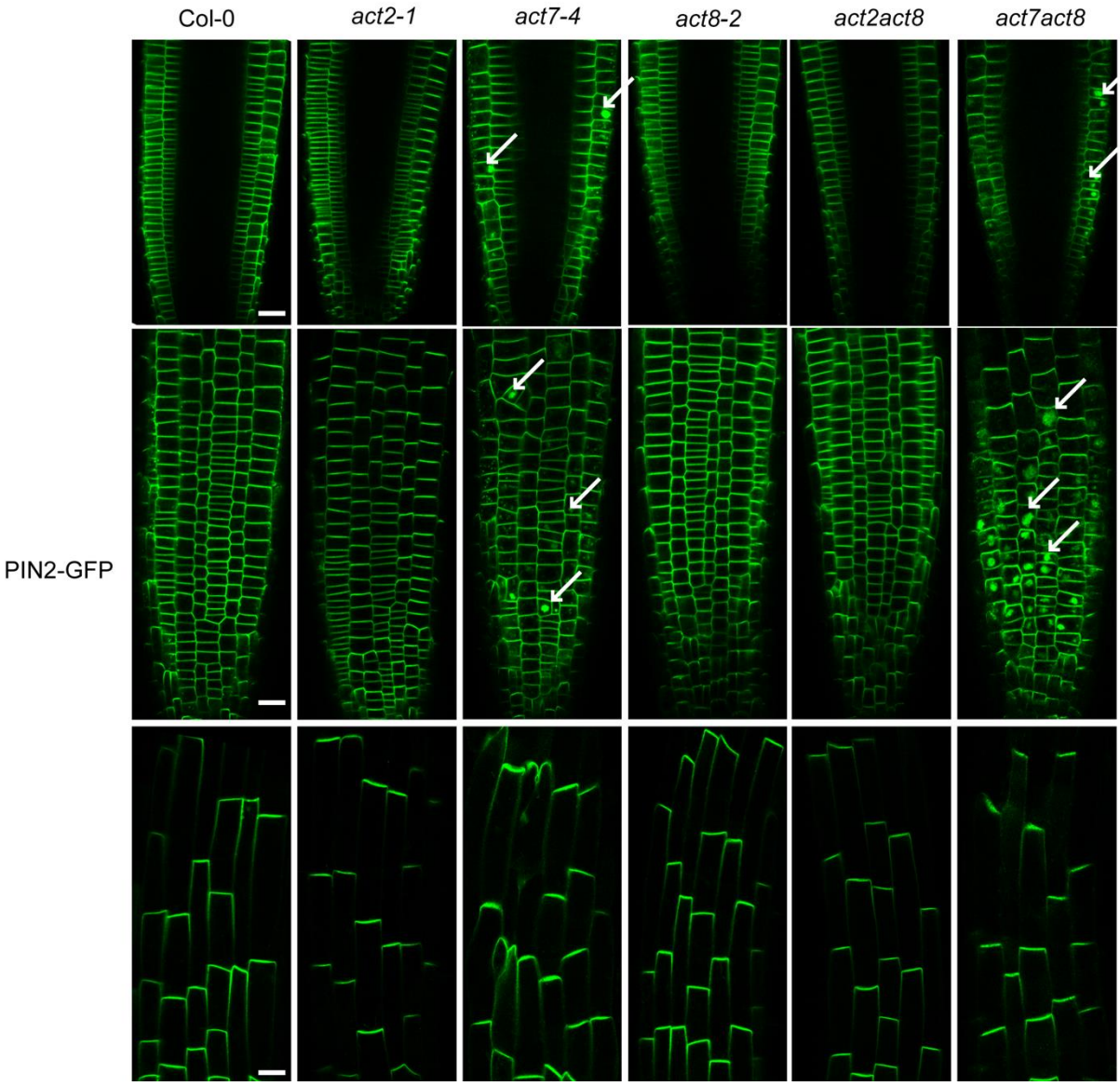

Figure 4. Loss of ACT7 but not ACT2 and ACT8 affects the intracellular dynamic cycling of PIN2.

Seven-day old PIN2:PIN2-GFP transgenic seedlings in wild-type and actin single and double mutant background were subjected to confocal imaging. The images were captured using the same confocal settings and are representative of 25 roots from three- four independent experiments. Upper and middle panel represent the images from the root meristem region. Lower panel represents the images from transition zone. The intracellular agglomeration of PIN2 was observed exclusively in the meristematic region of *act7* and *act7act8* mutants but not in the transition zone (Bottom Panel). Bars represent 10 μm.

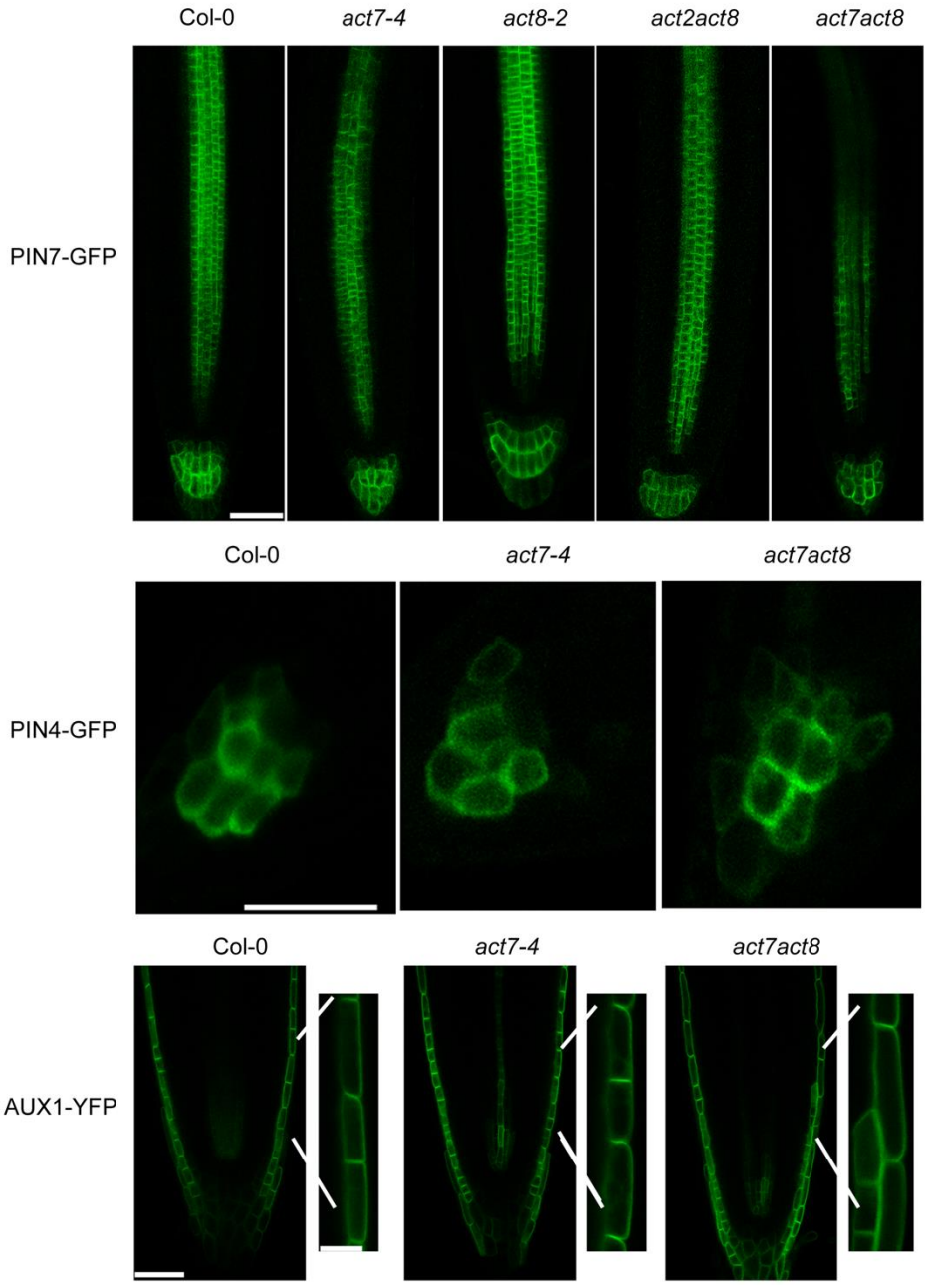

877

878 **Figure 5.** Effect of loss of ACT7 on PIN4, PIN7 and AUX1 expression

879 Seven-day old PIN7:PIN7-GFP, PIN4:PIN4-GFP, and AUX1-YFP transgenic seedlings in wild-
880 type and actin single and double mutant background were subjected to confocal imaging. The
881 images were captured using the same confocal settings and are representative of 20 roots from
882 three- four independent experiments. PIN7 expression was slightly reduced only in *act7act8*
883 mutants. PIN4 and AUX1 expression was unaltered in *act7* and *act7act8* mutants. Bars represent
884 10 mm. Bars represent 50 μm, and 10 μm for zoomed images of AUX1.

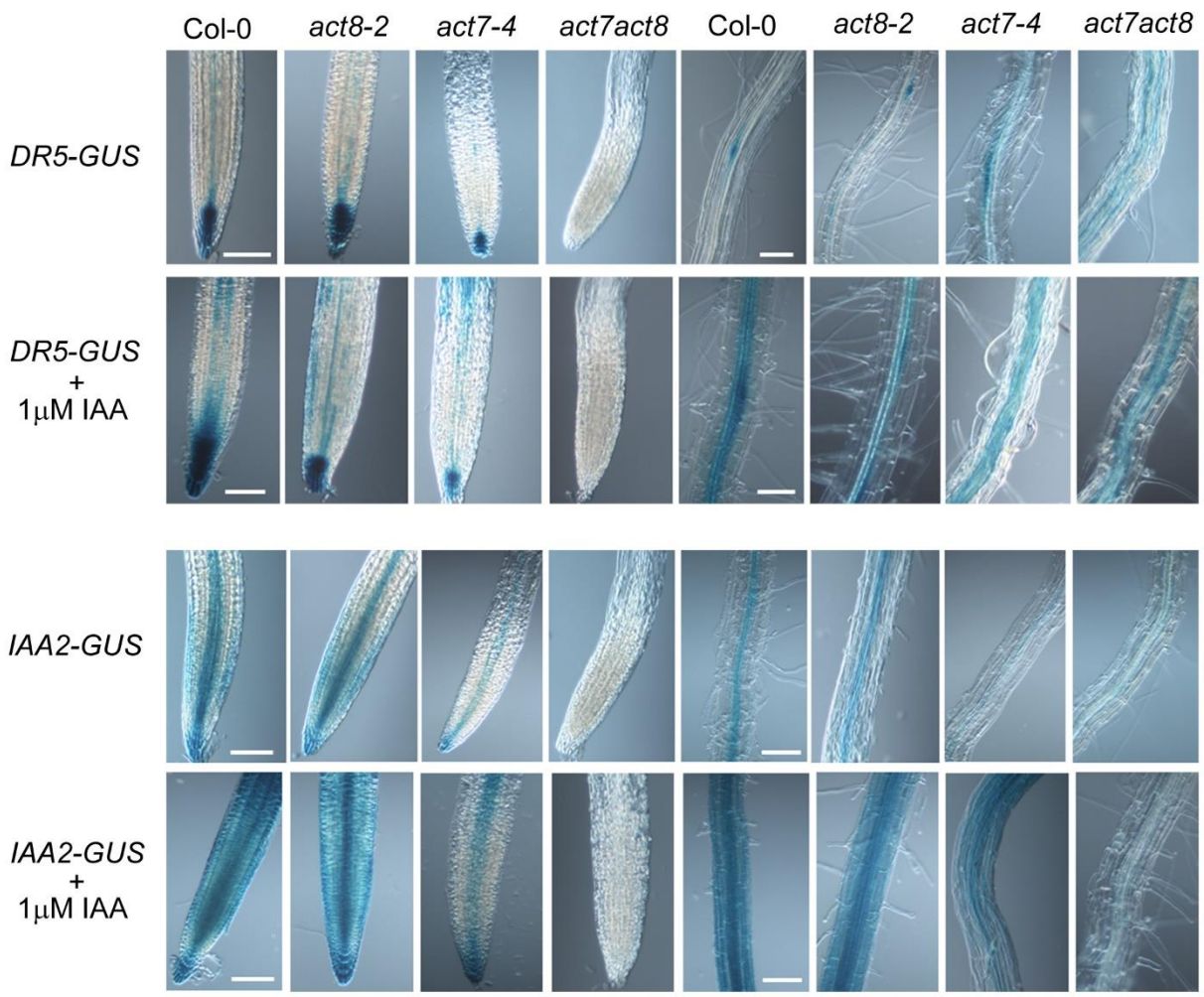

Figure 6. Effect of loss of actin isovariant on the root auxin gradient formation

Five-day old *DR5-GUS* and *IAA2-GUS* transgenic seedlings in wild-type and actin single and double mutant background were subjected to GUS staining. *DR5-GUS* transgenic seedlings were stained in buffer containing 1 mM X- gluc for 3 h and *IAA2-GUS* were stained for 1 h at 37°C. After the incubation, the roots were cleared for photography. Loss of ACT7 results in formation of reduced auxin gradient at root tip. Loss of both ACT7 and ACT8 further enhances the reduction. For exogenous auxin treatment the seedlings were incubated in 1μM IAA for 3h and subjected to GUS staining and cell clearing. The images are representative of 20 seedlings from three-four independent experiments. The results were confirmed with two separate lines for each crossing. Bars represent 100 μm.

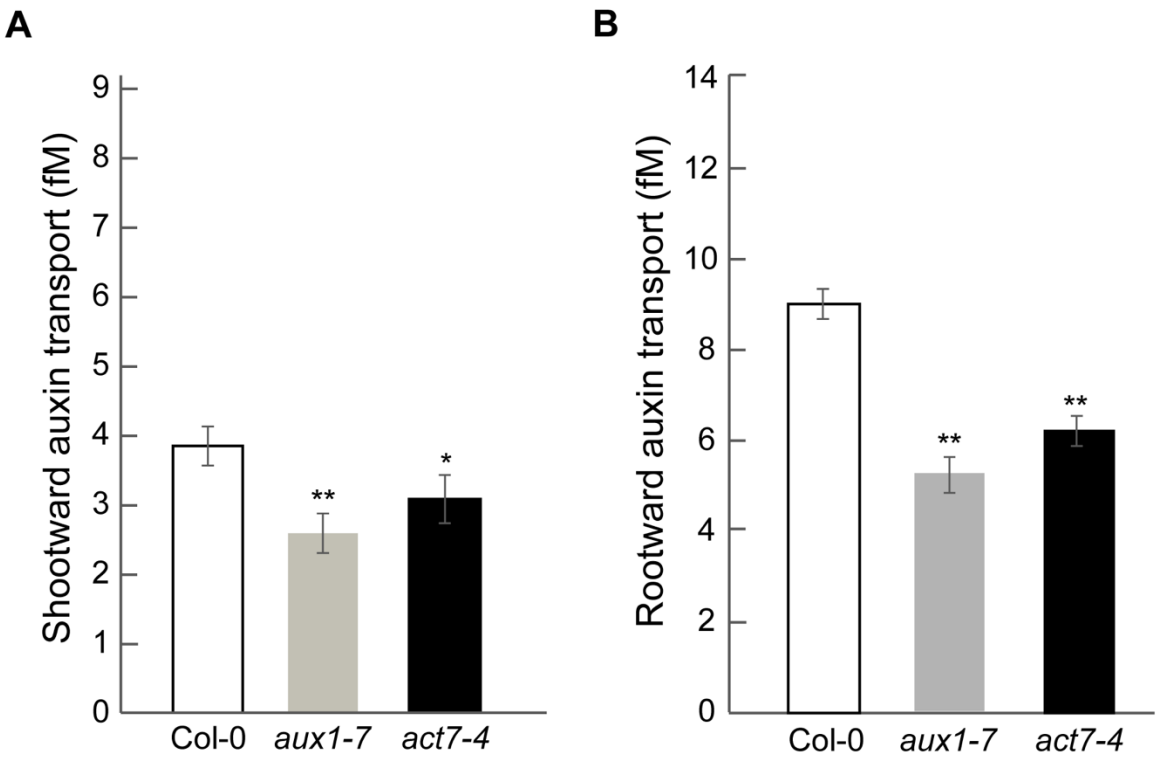

Figure 7. Auxin transport is disrupted in *act7* mutant.

Shootward and rootward auxin transport were measured using five-day-old seedlings. The experiments were performed in triplicate and repeated at least three times. Auxin influx facilitator mutant *aux1-7* was used as positive control. Asterisks represent the statistical significance between wild-type and mutants as judged by the Student`s *t*-test (*P<0.5, **P<0.01).

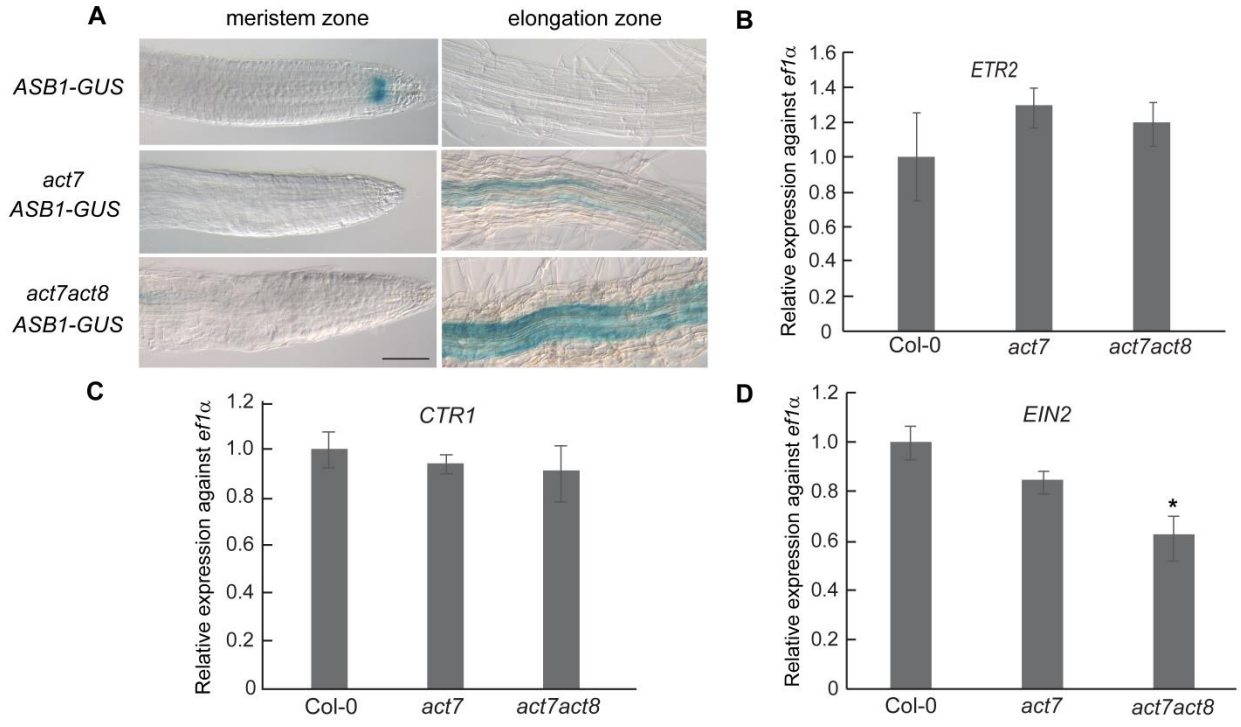

Figure 8. Molecular analysis of ethylene response in *act7* and *act7act8* mutants.

(C) Ectopic expression of ethylene-induced auxin biosynthesis gene *ANTHRANILATE SYNTHASE β1* in the mutants. The expression is reduced at the root tip but stimulated in the elongation zone. The images are representative of 20 seedlings from three independent experiments. Bars represent 50 μm.

(B-D) Expression analysis of the ethylene signaling genes in *act7* and *act7act8* mutants. qRT-PCR was performed using cDNA prepared from the root samples of five-day-old seedlings. All the data were normalized against *ef1α*. The data were obtained from three independent biological replicates. Asterisk represents the statistical significance between wild-type and mutants as judged by the Student`s *t*-test (*P<0.5).

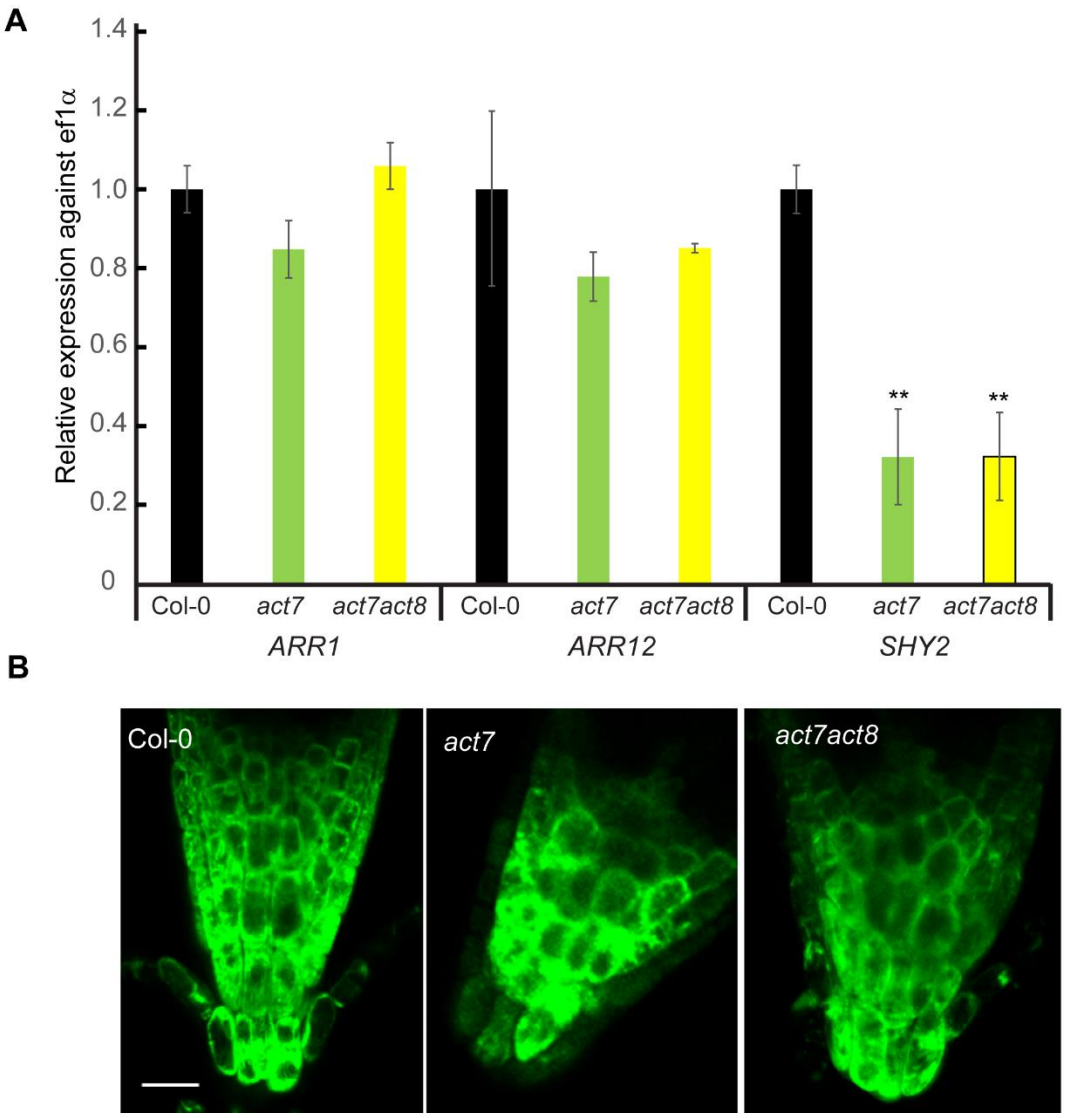

Figure 9. Molecular analysis of cytokinin responsive genes in *act7* and *act7act8* mutants.

(B) Expression analysis of the *ARR1*, *ARR12* and *SHY2/IAA3* in *act7* and *act7act8* mutants. qRT-PCR was performed using cDNA prepared from the root samples of five-day-old seedlings. All the data were normalized against ef1α. The data were obtained from three independent biological replicates. Asterisk represents the statistical significance between wild-type and mutants as judged by the Student`s *t*-test (**P<0.01).

(D) Expression of synthetic cytokinin marker *TCS-GFP* is not altered in *act7* and *act7act8* mutants. The images are representative of 20 seedlings from three independent experiments. Bar represents 50 μm.